



Elemental characterization of sparkling wine and cork stoppers

Rafaela Debastiani^{1,*}, Carla Eliete Iochims dos Santos², Johnny Ferraz Dias

Ion Implantation Laboratory, Institute of Physics, Federal University of Rio Grande do Sul, Av. Bento Gonçalves 9500, CP 15051, CEP 91501-970, Porto Alegre, RS, Brazil

ARTICLE INFO

Keywords:

PIXE
Elemental analysis
Sparkling wine
Wine aging
Cork stopper

ABSTRACT

The variations of the elemental concentrations in sparkling white wine and respective cork stoppers throughout 18 months of storage time were determined with the PIXE (Particle-Induced X-ray Emission) technique. Three portions of the cork stoppers were analyzed: the top part (external layer), the inner part (bulk layer) and the bottom layer (which was in contact with the sparkling wine). Elements such as Na, Mg, Si, P, S, Cl, K, Ca, Mn, Fe, Zn and Rb were determined for both cork stoppers and sparkling wine samples. Similar concentrations of Si, P, S, Cl and Ca were found in the external and bottom layers of the corks. Distinct behaviors of the changes in the elemental concentrations as a function of the time were observed for cork stoppers and sparkling wines. The concentrations of Mg, S, K, Ca, Cu, Sr and Ba increased in the bottom layer of the cork as a function of storage time. On the other hand, concentrations of Al, Si, Cl, Ti, Zn and Br proved to be invariant, while the concentrations of P and Fe showed a slight decrease. Concerning the sparkling wine, an increasing trend of elemental concentrations was observed for most elements throughout the storage time. A diffusion mechanism of elements in the cork and the role of the secondary fermentation in the bottle are discussed.

1. Introduction

With a production of about 3.1 million hectoliters of wine in 2018 (International Organisation of Vine and Wine, 2019), Brazil ranks 15th in the scenario of worldwide wine production. Despite the fact that sparkling wine represents a relatively small fraction of this production – less than 2% of the total wine production including table and fine wine (Mello, 2019) – its production has been steadily growing over the past years due to the increasing demand of local and export markets (Mello, 2019).

The quality of sparkling wines depends on several factors including the grape variety and the *terroir* since base wines carry not only intrinsic features of the soil but also bears signature of field practices and climate. Unlike regular wines, sparkling wines undergo a second fermentation either in the bottle or in appropriate tanks, where biochemical reactions and transformations occur due to the action of yeast cells during the aging (Sartor et al., 2019). Moreover, oenological agents are added to the process in order to impart stability and improve particular features

including taste and aroma. For instance, the addition of mannoproteins alters the organic composition of phenolic compounds and acids of rosé sparkling wine (Sartor et al., 2019). In this way, some properties of sparkling wines like effervescence and sugar content can reach an optimal balance thanks to these processes (Kemp et al., 2019).

The transformation of organic compounds and consequent changes of physico-chemical properties are relatively well documented for red wine (Cerdán et al., 2004; Jackson and Lombard, 1993; Chung et al., 2008) and sparkling wines during its aging period. Different techniques can be used in order to characterize sparkling wines regarding their total phenolics, proteins, polysaccharides and oligosaccharides contents among other important chemical parameters (Culbert et al., 2015, 2017; Martínez-Lapuente et al., 2018). On the other hand, there is no information whether its elemental profile changes as well due to the aging process and to the interactions with the cork stopper and with the glass bottle during this period. The present work tackles this very problem using a single technique for the analysis of wine and cork stoppers.

As far as elemental composition is concerned, techniques like

* Corresponding author. Institute of Nanotechnology, Karlsruhe Institute of Technology, Hermann-von-Helmholtz-Platz 1, 76344, Eggenstein-Leopoldshafen, Germany.

E-mail address: rafaela.debastiani@kit.edu (R. Debastiani).

¹ Institute of Nanotechnology, Karlsruhe Institute of Technology, Hermann-von-Helmholtz-Platz 1, 76344, Eggenstein-Leopoldshafen, Germany.

² Institute of Mathematics, Statistics and Physics, Federal University of Rio Grande, Campus Santo Antônio da Patrulha, Rua Barão do Café 125, CEP 95500–000, Santo Antônio da Patrulha (RS), Brazil.

<https://doi.org/10.1016/j.crfs.2021.09.006>

Received 28 May 2021; Received in revised form 2 September 2021; Accepted 18 September 2021

Available online 24 September 2021

2665-9271/© 2021 The Authors.

Published by Elsevier B.V. This is an open access article under the CC BY-NC-ND license

(<http://creativecommons.org/licenses/by-nc-nd/4.0/>).

Inductively Coupled Plasma Optical Emission Spectroscopy (ICP-OES) (Sartor et al., 2019; Rodrigues et al., 2020) and Atomic Absorption Spectroscopy (AAS) (Rizzon et al., 2009) have been employed for the analysis of sparkling and Chardonnay wines respectively. In brief, both ICP-OES and AAS are common techniques based on the emission and absorption of characteristic wavelengths, respectively, used for the quantitative determination of elemental composition of different samples including foodstuff. Another technique suitable for the elemental analysis of materials is the Particle-Induced X-ray Emission (PIXE) (Johansson et al., 1995). PIXE is a powerful technique based on the incidence of energetic protons on the sample. The ionization of the target atoms under proton bombardment may lead to the production of characteristic X-rays, thus allowing the identification and quantification of the elements present in the sample. PIXE is a multi-elemental non-destructive technique with limits of detection reaching few parts per million. Moreover, it provides relatively fast analysis requiring little sample handling depending on the material under analysis. These advantages lend versatility to this technique, which makes it useful for different fields including studies in biology and food science. Some examples include the study of wine (dos Santos et al., 2019), coffee (Cloete et al., 2019; Debastiani et al., 2019a, 2019b; Singh et al., 2020), tea (Giulian et al., 2007; Caniza et al., 2020) and wine stoppers (dos Santos et al., 2013) among others.

The goal of this work is to characterize sparkling white wines and their respective cork stoppers as a function of the storage time. In this way, to the present work aims at understanding the elemental profile changes due to the initial 18 months of the sparkling wine aging process and the effects of the interactions with the cork stopper and with the glass bottle during this period.

2. Materials and methods

2.1. Samples

The samples of sparkling wine were obtained from a winery located at Vale dos Vinhedos, Serra Gaúcha, which is the leading wine production region of Rio Grande do Sul state in Southern Brazil. The wine consisted of a blend made of Chardonnay and Pinot Noir grape varieties and was elaborated according to the champenoise method, also known as “traditional method”. In this case, the second fermentation of the base wine takes place in the bottle. To that end, a mixture of sugars and yeast (the so-called *liqueur de tirage*) (Joshi, 2011) is added to the wine prior to sealing the bottle with a cork stopper.

In order to evaluate the elemental composition of the wine as a function of the storage time, 7 groups of 5 bottles each of sparkling wine were analyzed. The bottling date corresponds to the point in time where all bottles were filled up with the sparkling wine extracted from the tank in the winery. Five bottles were separated and were not sealed with any cork. In this case, the wine did not have any contact with the corks. These samples are referred to as “G1” and correspond to the initial collection time. These samples were immediately prepared for PIXE analysis. In this way, G1 samples did not undergo through the second fermentation (which takes about 2 months to be completed after sealing the bottle) and aging (Joshi, 2011) in the bottle. Five pristine corks were also analyzed without any previous contact with wine. The other bottles were sealed with cork stoppers (Fig. 1) and were carefully transported to the laboratory where they were stored in a shelf in the horizontal position without luminosity. The room was kept under at a temperature of (24 ± 2) °C and a humidity level of $(55 \pm 5)\%$.

Every three months, wine samples from five bottles and their respective corks were prepared for analysis (Table 1). These samples correspond to G2 (3 months of storage time) up to G7 (18 months of storage time). Three samples were prepared per bottle, thus totaling 15 samples per group.

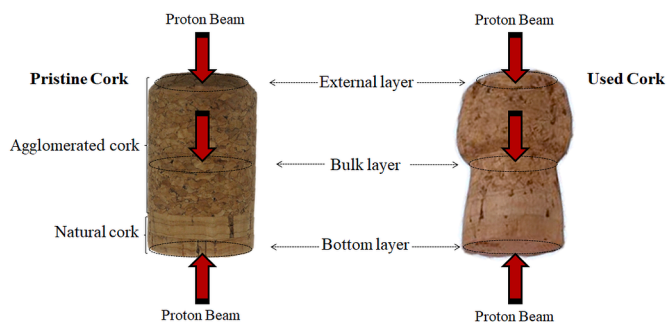


Fig. 1. Pristine cork stopper (left panel) made of two disks of natural cork (bottom) and agglomerated cork (middle and top portions). The right panel depicts the used corks. The external and bulk layers had no direct contact with the wine, while the bottom layer was in direct contact with the wine during the storage time. The oval dashed lines are used for better visualization of the structures under discussion. The red arrows indicate the direction of the proton beam during the PIXE analysis. (For interpretation of the references to colour in this figure legend, the reader is referred to the Web version of this article.)

Table 1

Nomenclature of the sample groups according to the storage time.

Group Name	Storage Time (months)
Group 1 (G1)	0
Group 2 (G2)	3
Group 3 (G3)	6
Group 4 (G4)	9
Group 5 (G5)	12
Group 6 (G6)	15
Group 7 (G7)	18

2.2. Sparkling wine

Due to characteristics of the PIXE technique (Johansson et al., 1995), the samples must be dry, homogeneous and have a smooth surface. Thus, the sparkling wine samples were prepared according to the protocol developed by dos Santos et al. (dos Santos et al., 2010). In short, 500 mL of wine were collected from each bottle and dried at 150 °C in an oven for about 9 h. The residues were then removed from the beaker and homogenized with a mortar and pestle. Finally, the powder was pressed into 2 mm thick pellets of 0.25 g and 13 mm of diameter.

2.3. Cork stopper

The cork stoppers used in this work were provided by the winery without any further information. They consist of two layers of natural cork followed by a large portion of agglomerated cork. Different types of adhesives are used to glue together the natural cork disks and the agglomerated portion of the cork (Six and Feigenbaum, 2003). Following a particular protocol detailed elsewhere (dos Santos et al., 2013), three samples were prepared for each cork stopper by cutting 2 mm thick disks in different parts of the cork as shown in Fig. 1: external layer (upper part of the cork stopper); bulk layer (middle part of the cork stopper); and bottom layer (lower part of the cork stopper consisting of natural cork in direct contact with the wine). The external and bulk layers represent the agglomerated portions of the cork. The same three parts were analyzed for pristine cork stoppers (without any contact with the wine – G1 group), in order to characterize them from the elemental point of view. In total, 5 samples of external, bulk and bottom layers were prepared for each of the seven groups shown in Table 1, thus totaling 15 cork samples per group. After the bottles were opened, the corks were left to dry at room temperature. Despite cork stoppers are highly inhomogeneous (dos Santos et al., 2013), only one spot was measured for each of the samples since 5 independent measurements

were carried out for each group and for each sample category (external, bulk and bottom layers). Moreover, the relatively large beam spot size used during the experiments (9 mm^2) ensures that different inhomogeneities are irradiated at the same time, thus providing an X-ray spectrum representative of different structures within the cork.

2.4. PIXE instrumentation

PIXE experiments were carried out at the Ion Implantation Laboratory of the Federal University of Rio Grande do Sul. A Tandem accelerator delivered a 2 MeV proton beam at the PIXE station for the elemental analysis. The samples were accommodated in a ladder placed inside the reaction chamber. The samples were positioned in the proton beam through an electromechanical system coupled to a CCD camera for visualization. The reaction chamber was kept under a pressure of the order of 10^{-6} mbar throughout the experiments. Moreover, the reaction chamber is completely insulated from the accelerator and other electrical devices, thus allowing a direct measurement of the total charge collected during the experiments. Each sample was irradiated during 400 s with an average current of 3 nA. The beam spot size on the samples was about 9 mm^2 . Such broad beam minimizes the influence of inhomogeneities in the samples. The characteristic X-rays induced in the samples were detected by a Si(Li) detector placed at -135° with respect to the beam direction. The energy resolution of the detector is about 150 eV at 5.9 keV while its efficiency reaches 90% for 2 keV photons (Fernandes et al., 2018).

The PIXE system is calibrated with several NIST (National Institute of Standards and Technology) and Micromatter® certified materials. In the present work, apple leaves standard (NIST reference material 1515) was chosen for the calibration of the system and for obtaining the recovery values due to its similarity to the sparkling wine matrix (Debastiani et al., 2019b).

2.5. Data analysis

The X-ray spectra were analyzed with the GUPIXWIN software package (Campbell et al., 2000). The software performs a least-square fitting procedure of all X-ray peaks simultaneously. All experimental parameters including geometric factors and the detector's solid angle are taken into account during the analysis. Moreover, thick target effects like X-ray self-absorption and secondary fluorescence are included in the analysis as well. Finally, X-ray peak areas are converted to elemental concentrations through the experimental and physical parameters like X-ray production cross sections and stopping powers. The results for the elemental concentrations are given as part per million (ppm) dry weight.

The final concentrations of the elements were quoted for each group from the average of those values above the limit of detection (LOD). For the comparison among different groups of sparkling wine and cork stoppers, the one-way analysis of variance (ANOVA) and Tukey's post hoc tests (significance level of 0.05) were performed using the SPSS® software. For the analysis of deposition rates in the wine and on the bottom layers of the corks a linear regression analysis was carried out and the statistical significance of the population slope was tested with the F test with a level of significance of 0.05.

3. Results and discussions

3.1. Recovery values

The quality of the PIXE system is assessed through the recovery values obtained through periodic calibrations of the system with reference materials. In the present study, the recovery values were obtained through the analysis of apple leaves standard (NIST reference material 1515). The results vary from 1.6% for magnesium up to 7.0% for iron, with values of 2.1% for potassium, 2.4% for calcium and 4.8% for zinc. The recovery values for other elements can be found elsewhere

(Debastiani et al., 2019b).

3.2. Elemental composition of cork stoppers

Fig. 2 shows representative X-ray spectra of pristine cork stoppers belonging to the G1 group. The first remarkable feature one can observe is the similarity between the bottom and external layers. Despite the bottom layer is made of natural cork while the external layer consists of agglomerated cork, this similarity may reflect the external treatment with silicone resins corks usually undergo in order to improve their sealant properties. The prominent silicon peak is just a consequence of this treatment. Other elements including titanium and iron might be related with this treatment as well since their concentrations are greatly reduced in the bulk layer. Besides Si, other elements like P, S, Cl and Ca have similar concentrations in these parts of the corks. These results agree with those published elsewhere (Ortega-Fernández et al., 2006; dos Santos et al., 2013). It is important to note that differences observed on the bottom layer when compared to other layers of the cork could stem from the interaction of the wine with the bottom layer. Despite intrinsic inhomogeneities of the corks cannot be discarded as a potential source of differences (dos Santos et al., 2013), the use of a broad proton beam minimizes the influence of such inhomogeneities on the final results.

The mean elemental concentrations of the bottom, bulk and external layers of corks from all groups are shown in Table 2. This table reveals that some elements like Rb, Sr and Ba were found in concentrations above the limit of detection (LOD) in few external layer samples. Elements like Al, Ti, and Cr showed up in few bulk layer samples, while Rb and Sr were not detected in any of the samples from this layer. Finally, Ni was found in only 1 sample of the bulk and bottom layers. In general, the elemental concentrations shown in Table 2 for the bulk layer are higher than those reported by dos Santos et al. (dos Santos et al., 2013), thus suggesting that the corks used in both studies are quite distinct. Most surprisingly is the presence of Ba found in 10 samples of the bulk layer and in 29 samples of the bottom layer, which was not reported in the work of dos Santos et al. (dos Santos et al., 2013). Since the sample preparation protocol for corks is quite simple with practically no handling of the samples, we can discard any kind of contamination. However, the presence of Ba in cork slabs and cork granules has already been reported with concentrations varying from $6.2 \pm 0.2 \text{ mg}\cdot\text{kg}^{-1}$ up to $142 \pm 6 \text{ mg}\cdot\text{kg}^{-1}$ respectively (Corona et al., 2014). Moreover, the sparkling wine corks are composed by an agglomerated body glued to two disks of natural cork. The assemble of the agglomerated part and the gluing of the natural cork parts can be carried out using polymer-based adhesives like polyurethane (Six and Feigenbaum, 2003). Usually, this adhesive can have its mechanical and chemical properties improved by the addition of inorganic fillers as barium sulfate (Shahzamani et al., 2012). Since the bottom layer of the cork is in direct contact with the liquid, the wine can penetrate into the cork increasing the surface of contact and diffusion of material from the adhesive to the cork parts could take place (Six et al., 2002). The large amount of sulfur on the bottom layer of the cork (Table 2) could be due to the diffusion of barium sulfate from the cork and to the absorption of sulfur from the wine since it contains sulfites.

The results of the bottom layer of the cork stoppers as a function of the storage time indicate that the concentrations of Al, Si, Cl, Ti, Zn and Br are invariant, while the concentrations of P and Fe show a slight decrease over time. The concentrations of the remaining elements display a rising trend as shown in Fig. 3. Indeed, the concentrations of Mg, S, K, Ca, Cu, Sr and Ba are consistent with a steady deposition growth on the bottom layer of the cork. Table 3 shows the deposition rate of these elements per month. Both Ba and S are elements with the highest deposition rate, namely 277 and $89 \text{ mg}\cdot\text{kg}^{-1}$ per month respectively.

The deposition of elements on the surface of the corks' bottom layer may be the result of two distinct process: 1) absorption of elements from

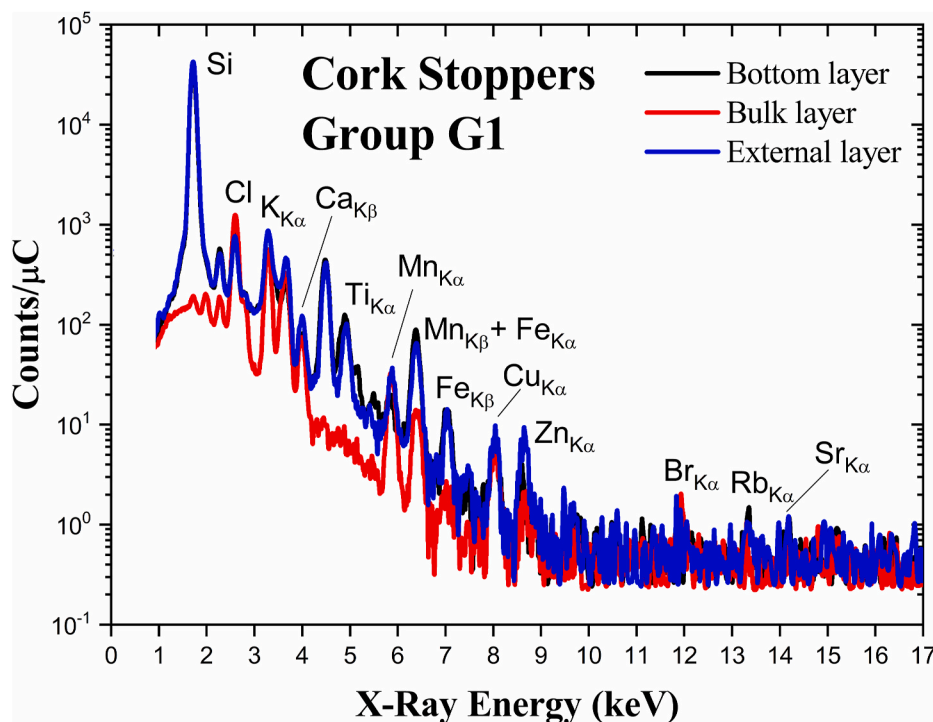


Fig. 2. X-ray spectra of bottom (black line), bulk (red line) and external (blue line) layers of pristine cork stoppers belonging to G1 group as a function of the X-ray energy. Each spectrum represents an average of 5 measurements. All spectra are normalized by the charge accumulated during the experiments. (For interpretation of the references to colour in this figure legend, the reader is referred to the Web version of this article.)

Table 2

Elemental concentrations of the external, bulk and bottom layers of cork stoppers. The values and uncertainties are represented by the mean and the standard deviation of the mean respectively. The averages refer to all “n” samples from all groups whose results were above the limit of detection (LOD). All data are expressed in $\text{mg}\cdot\text{kg}^{-1}$.

Element	External Layer (n)	Bulk Layer (n)	Bottom Layer (n)
Na	514 ± 99 (12)	118 ± 47 (8)	161 ± 16 (4)
Mg	145 ± 19 (9)	156 ± 25 (13)	278 ± 28 (7)
Al	229 ± 19 (30)	59 ± 13 (2)	292 ± 22 (34)
Si	51273 ± 6311 (33)	132 ± 33 (31)	70970 ± 7211 (33)
P	195 ± 28 (19)	246 ± 19 (33)	169 ± 18 (16)
S	880 ± 50 (35)	257 ± 20 (34)	1497 ± 114 (34)
Cl	2567 ± 203 (34)	2817 ± 192 (34)	2263 ± 228 (34)
K	2206 ± 277 (34)	2142 ± 238 (33)	1067 ± 66 (34)
Ca	696 ± 93 (34)	579 ± 80 (31)	552 ± 104 (34)
Ti	172 ± 22 (34)	15.7 ± 10.9 (4)	313 ± 26 (34)
Cr	4.3 ± 0.5 (13)	2.9 ± 0.6 (4)	3.1 ± 0.7 (6)
Mn	18.7 ± 3.2 (34)	18.3 ± 2.1 (30)	8.8 ± 1.1 (9)
Fe	41.5 ± 6.1 (35)	6.7 ± 0.9 (32)	28.4 ± 2.1 (33)
Ni	2.2 ± 0.3 (10)	1.03 (1)	2.3 (1)
Cu	10.5 ± 0.7 (33)	9.2 ± 0.5 (34)	13.1 ± 1.3 (32)
Zn	11.8 ± 2.7 (24)	4.4 ± 1.1 (7)	6.4 ± 0.9 (18)
Br	12.1 ± 1.3 (12)	10.6 ± 0.6 (8)	10.2 ± 2.1 (8)
Rb	13.2 (1)	–	8.7 ± 2.5 (5)
Sr	24.1 ± 3.8 (3)	–	122 ± 19 (25)
Ba	66 ± 43 (2)	38.6 ± 17.1 (10)	2473 ± 332 (29)

the sparkling wine due to the contact of the cork with the liquid during the process of fermentation. This process could contribute to the concentrations of elements like potassium and sodium (Kemp et al., 2019) since tartaric acid from the wine could accumulate in the corks’s surface in the form of salts; 2) diffusion of elements from inner parts of the cork towards its surface through the wet portion of the cork. While absorption indicates a direct transfer of elements from the sparkling wine to the cork, a diffusion process suggests that the sparkling wine plays no role in the deposition other than providing a fluid medium to facilitate such

diffusion. Finally, it is important to bear in mind that PIXE is essentially a near-surface technique and therefore provides elemental concentrations from very thin portions of the structure under study. For instance, if we assume that the coating treatment of the cork and the cork itself are made of paraffin wax and cellulose respectively, then 2.0 MeV protons would penetrate about $(71 \pm 3) \mu\text{m}$ in the coating and $(53 \pm 2) \mu\text{m}$ in the cork (Ziegler, 1977).

3.3. Elemental composition of sparkling wine

Fig. 4 shows a typical PIXE spectrum of the sparkling wine. The spectrum is dominated by the presence of K and Ca with substantial contributions of P and S. Elements like Al, Ti, Cu, Br and Sr were detected only in some of the samples studied along the 18 months of storage time. Indeed, Sr was detected above the LOD in 4 samples only from G3 and G5 groups each with average concentrations of $(0.56 \pm 0.09) \text{mg}\cdot\text{L}^{-1}$ and $(0.47 \pm 0.14) \text{mg}\cdot\text{L}^{-1}$ respectively. Copper was found in 11 samples only from G7 group with an average concentration of $(0.066 \pm 0.014) \text{mg}\cdot\text{L}^{-1}$. Finally, Ba was not detected in any of the samples.

The average concentrations of the remaining elements as a function of the storage time are shown in Table 4. In general, the elemental concentrations shown in this table for Mg, Ca and K belonging to the G5 group are lower than those reported by Sartor et al. (2019) for 12 months aged wine, while the concentration of Mn is slightly higher in our study. The most striking result corresponds to the K concentration, which corresponds to about half of the values presented by Sartor et al. (2019). However, this may be related to the origin of the wine, to the grape variety, to the blend of different varieties and to field and producing practices. While our samples correspond to sparkling white wine produced through a blend of Chardonnay and Pinot Noir grape varieties from the Serra Gaúcha region (Rio Grande do Sul state), Sartor’s results refer to sparkling rosé wine produced with Merlot grapes from a different region (Santa Catarina state). Another study carried out by Rizzolo et al. (2018) found a much higher K concentration in sparkling

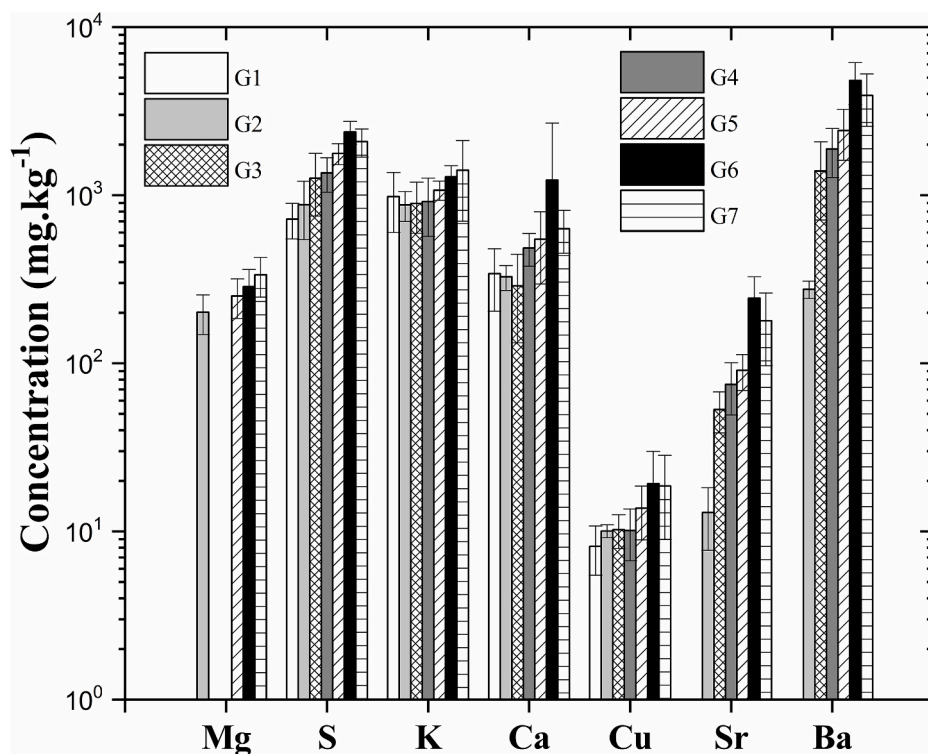


Fig. 3. Concentrations of Mg, S, K, Ca, Cu, Sr and Ba in the bottom layer of the cork stopper along 18 months of storage time in steps of 3 months. G1 group represents those corks which did not interact with the sparkling wine, i.e. equivalent to zero months of storage time. The values stand for the mean of five samples per group, while the uncertainties are represented by the standard deviation. Magnesium was not detected in G1, G3 and G4 groups, while Sr and Ba were absent from G1 samples.

Table 3
Elemental deposition rates on the bottom layer of the cork.

Element	Deposition Rate (mg.kg ⁻¹ .month ⁻¹)
Mg	7.8 ± 1.5
S	89 ± 9
K	26.1 ± 6.6
Ca	20.0 ± 4.5
Cu	0.38 ± 0.12
Sr	10.4 ± 1.5
Ba	277 ± 27

red wine produced with Merlot, Pinot Noir, Teroldego and a blend of these grape varieties than that reported by Sartor et al. (2019). Finally, a study of the Merlot wine from Rio Grande do Sul by Rizzon and Miele found the K concentration in the range between 1161 and 1372 mg.L⁻¹ (Rizzon and Miele, 2009).

Table 5 compares our PIXE results with those obtained with the ICP-OES technique reported by Rodrigues et al. (2020) for sparkling white wine and with the AAS technique reported by Rizzon et al. (2009) for Chardonnay wine. Both results refer to wines produced in the same region of Rio Grande do Sul. These results were converted to mg per glass of wine assuming that one glass is equivalent to 150 mL. This conversion allows us to compare the elemental intake per glass of wine with the Recommended Dietary Allowances (RDA) and the Tolerable Upper Intake Levels (TUIL) set by the United States Department of Health & Human Services (NIH, 2020). Our results for macronutrients like Na and Mg are lower than those reported by Rodrigues (Rodrigues et al., 2020), Rizzon (Rizzon et al., 2009) and Sartor (Sartor et al., 2019), while our result for Zn is higher than those quoted by Rizzon (Rizzon et al., 2009) and Sartor (Sartor et al., 2019). All studies but that carried out by Sartor indicate about the same concentration of K. Finally, all results suggest that the consumption of one glass of wine per day can be considered safe according the RDA and TUIL recommendations.

Table 4 indicates that sparkling wine samples coming from G1 group (wine before bottling) differs from at least one of the other periods of storage for all the analyzed elements. In general, all elements but Mg and

Si show a rising trend for their concentrations as a function of the storage time. Although the concentration of Si is very high in the cork stoppers (Table 2), it seems that it does not affect the sparkling wine since its concentration remained constant over time at relatively low levels. Table 4 reveals that Mg and P presented an increase in their concentrations up to G4 and G5 respectively, and then a decrease in the concentration up to G7. The concentration of Fe varied from 0.36 mg.L⁻¹ up to 0.92 mg.L⁻¹, in a sequence of an up-and-down fluctuation.

In order to investigate the rising trend of the concentrations of some elements as a function of time, a linear regression analysis was carried out and the slope was checked with the F test taking into account a level of significance of 0.05. As an example, Fig. 5 shows the Na concentration as a function of the aging time extracted from Table 4. The rising trend of the Na concentration is clearly visible. Similar analysis was carried out for all elements and the results are shown in Table 6. Interestingly, elements such as S, K and Ca increase their concentration in both sparkling wine and cork, suggesting that different potential sources of these elements with different dynamic transfers could be at play simultaneously. As far as the sparkling white wine is concerned, one of them would be the cork itself through the dissolution of elements from its bottom layer to the wine. Another potential source for these elements could be the wine bottles themselves. Usually, foodstuff in general and wine in particular contain sulfites (EFSA, 2016b) in order to preserve its quality for longer times due to its sanitizing properties. Moreover, wine bottles can be sanitized with e.g. sodium (Na₂S₂O₅) and potassium (K₂S₂O₅) metabisulfites (EFSA, 2016a). If residues of the sanitizing procedure are leftover to dry inside the bottle prior to wine bottling, they could be released overtime to the wine inside the bottle. Although this hypothesis cannot be ruled out, its contribution to the increase of some elemental concentrations in wine is estimated to be small.

A third potential source of elements is the secondary fermentation in the bottle and the subsequent wine aging. Indeed, it is important to bear in mind that the bottles of the present study were sealed after the addition of the *liqueur de tirage* (Joshi, 2011) made of yeast (*Saccharomyces cerevisiae*) and sugars required for the secondary fermentation in the bottle. The yeast is rich in elements like K (ca. 20 mg.g⁻¹) and P (ca.

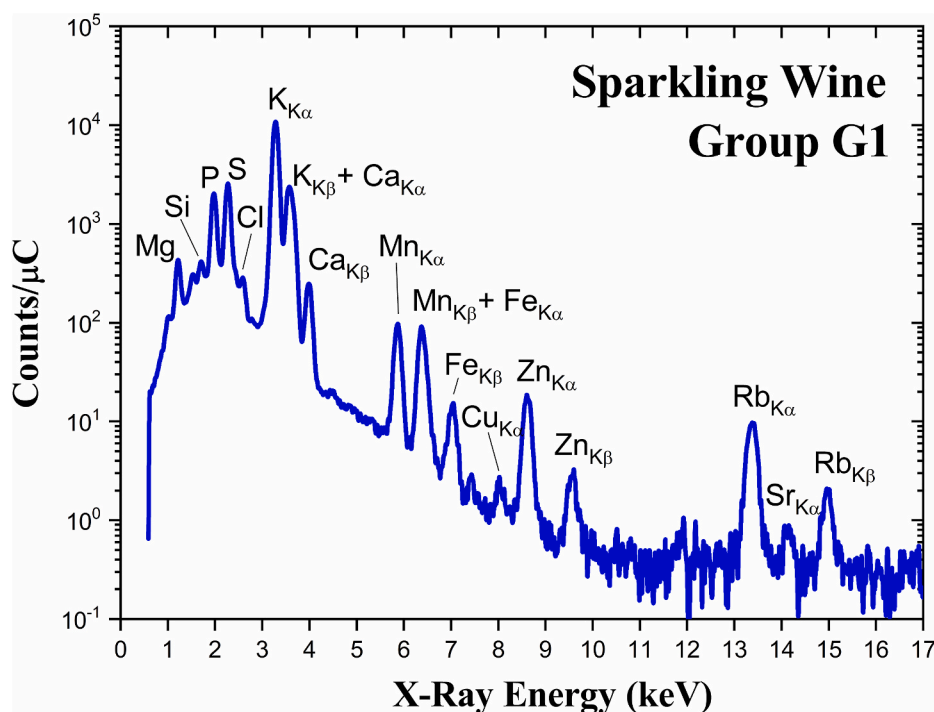


Fig. 4. X-ray spectrum of sparkling wine belonging to G1 group as a function of the X-ray energy. This spectrum represents an average of 5 measurements. The spectrum is normalized by the charge accumulated during the experiments.

Table 4

Elemental concentrations of the sparkling white wine. The values and uncertainties are represented by the mean and the standard deviation respectively. All data are expressed in $\text{mg}\cdot\text{L}^{-1}$. Equal superscript letters in the same row represent statistically significant equality between the values ($p < 0.05$).

	G1	G2	G3	G4	G5	G6	G7
Na	10.0 ± 2.4 ^a	13.6 ± 3.1 ^{ab}	11.9 ± 3.9 ^{ac}	12.3 ± 2.3 ^{ad}	15.4 ± 4.3 ^{bcd}	18.1 ± 2.7 ^e	16.3 ± 4.5 ^{bde}
Mg	42.9 ± 6.4 ^a	44.0 ± 9.8 ^{ab}	49.6 ± 13.2 ^{abc}	62.6 ± 5.0 ^d	54.3 ± 3.1 ^{cdef}	59.0 ± 9.3 ^{deg}	51.9 ± 3.7 ^{bfg}
Si	10.5 ± 0.8 ^a	10.7 ± 1.3 ^a	10.2 ± 1.2 ^a	8.6 ± 1.2 ^b	10.0 ± 0.6 ^a	10.3 ± 1.1 ^a	10.9 ± 1.0 ^a
P	102 ± 8 ^a	106 ± 11 ^a	108 ± 15 ^{ab}	119 ± 7 ^c	131 ± 6 ^{de}	124 ± 7 ^{ce}	117 ± 5 ^{bc}
S	77 ± 7 ^a	87 ± 13 ^{ab}	92 ± 14 ^b	97 ± 8 ^{bc}	104 ± 6 ^c	128 ± 7 ^d	121 ± 7 ^d
Cl	9.2 ± 1.4 ^a	10.2 ± 1.3 ^{ab}	9.9 ± 1.5 ^{ab}	11.1 ± 0.8 ^b	13.7 ± 0.9 ^c	13.7 ± 0.8 ^c	12.8 ± 1.1 ^c
K	481 ± 68 ^a	494 ± 76 ^a	332 ± 77 ^b	503 ± 102 ^a	629 ± 61 ^c	602 ± 138 ^c	674 ± 20 ^c
Ca	33.7 ± 9.3 ^{ab}	30.2 ± 9.8 ^{bc}	44.0 ± 13.0 ^{ad}	35.6 ± 10.2 ^{ace}	40.6 ± 9.0 ^{bde}	49.0 ± 7.3 ^d	49.7 ± 7.3 ^d
Mn	1.31 ± 0.16 ^a	1.30 ± 0.26 ^a	1.53 ± 0.3 ^{ab}	1.76 ± 0.13 ^{bc}	1.71 ± 0.10 ^{bc}	1.90 ± 0.30 ^c	1.87 ± 0.12 ^c
Fe	0.36 ± 0.05 ^a	0.90 ± 0.28 ^b	0.48 ± 0.14 ^{acd}	0.78 ± 0.21 ^b	0.52 ± 0.05 ^{acd}	0.73 ± 0.17 ^{bd}	0.92 ± 0.36 ^b
Zn	0.62 ± 0.07 ^{ab}	0.67 ± 0.12 ^{ac}	0.79 ± 0.17 ^{cd}	0.74 ± 0.08 ^{bce}	0.81 ± 0.07 ^{de}	0.90 ± 0.10 ^d	0.88 ± 0.15 ^d
Rb	2.32 ± 0.42 ^a	2.27 ± 0.43 ^a	1.84 ± 0.47 ^a	3.10 ± 0.62 ^b	3.20 ± 0.57 ^b	3.31 ± 0.78 ^b	3.61 ± 0.61 ^b

15 $\text{mg}\cdot\text{g}^{-1}$) among others (Halász and Lásztity, 1991; Yamada and Sgarbieri, 2005). Despite the secondary fermentation is a relatively fast process (about two months), the release of compounds and elements from yeast after autolysis (yeast lees) is slower due to the cell wall degradation process (Fornairon-Bonnefond et al., 2002). This mechanism, frequently referred to wine aging, is very important because it imparts new characteristics to the wine due to the release of compounds and elements to the beverage. This process might be responsible for the

increase of some elemental concentrations in wine as a function of the time.

4. Concluding remarks

In this work, the elemental compositions of sparkling white wine and their respective cork stopper were studied as a function of the storage time using the PIXE technique. Each cork stopper was sampled in three distinct portions, namely external, bulk and bottom layers, the latter being the one in contact with the sparkling wine. The external and bottom layers of the cork are characterized by the presence of Si due to the resin treatment of the cork. Other elements like Ti, Fe, Ni and Zn could be related to the resin treatment as well since their presence in the bulk layer are greatly reduced in terms of concentration and/or number of samples where they were detected. Several samples of the bulk and bottom layers contained Ba, which is a relatively rare element and therefore straightforward to be identified. Despite Ba was not observed in our previous work with corks (dos Santos et al., 2013), it was found in Spanish cork (Corona et al., 2014) and recently in Marselan wines (dos Santos et al., 2019). Furthermore, BaSO_4 can be present in the adhesive (polyurethane) used to glue the natural cork layers together and to the agglomerated portion of the cork.

Seven elements (Mg, S, K, Ca, Cu, Sr and Ba) increased their concentrations in the bottom layer of the corks as a function of the storage time with depositions rates varying from 0.38 $\text{mg}\cdot\text{kg}^{-1}$ per month for Cu up to 277 $\text{mg}\cdot\text{kg}^{-1}$ per month for Ba. Most of these elements belong to the group II of the periodic table (Mg, Ca, Sr and Ba) and therefore have reduced power of solubility in various forms (sulfates, hydroxides and carbonates). However, this fact does not rule out a diffusion process of these elements from the adhesive or from deeper portions of the bottom layer towards its surface using wine moisture as a facilitator vehicle.

The elemental concentrations of the sparkling wine show a rising trend for all elements but Mg and Si as a function of the storage time. The rising trend of the elemental concentrations in the wine could in part stem from the bottom layer of the cork since all these elements are present in this layer. However, S, K and Ca also increase their

Table 5

Elemental concentrations of sparkling white wines (G7 group of this work and results from Rodrigues et al., 2020), Chardonnay wine (Rizzon et al., 2009) and sparkling rosé wine (Sartor et al., 2019). The wine results are given in units of mg per glass of wine assuming that one glass is equivalent to 150 mL. The Recommended Dietary Allowance (RDA) represents the average daily intake sufficient to meet the nutrient requirements of nearly all healthy people. The Tolerable Upper Intake Level (TUIL) represents the maximum daily intake unlikely to cause adverse health effects. The RDA and TUIL data were extracted from NIH (2021) and are given in units of mg per day.

	G7 Sparkling White Wine (This Work) (mg/glass)	Recommended Dietary Allowances (mg/day)	Tolerable Upper Intake Levels (mg/day)	Chardonnay Wine (Rizzon et al., 2009) (mg/glass)	Sparkling White Wine (Rodrigues et al., 2020) (mg/glass)	Sparkling Rosé Wine (Sartor et al., 2019) (mg/glass)
Na	2.44 ± 0.68	1500*	ND	4.8	6.6	NA
Mg	7.78 ± 0.56	362	350**	11.6	10.5	9.9
P	17.58 ± 0.74	700	4000	13.8	NA	NA
K	101 ± 3	3000*	ND	106	102	172
Ca	7.46 ± 1.10	1000	2500	13.0	13.2	9.5
Mn	0.28 ± 0.02	2.05*	11	0.42	0.24	0.21
Fe	0.13 ± 0.05	13	45	0.3	0.21	0.16
Zn	0.13 ± 0.02	9.5	40	0.09	NA	0.80

ND: Not Determinable.

NA: Not Available.

* Adequate Intake (AI): established when evidence is insufficient to develop an RDA and is set at a level assumed to ensure nutritional adequacy.

** Supplemental magnesium.

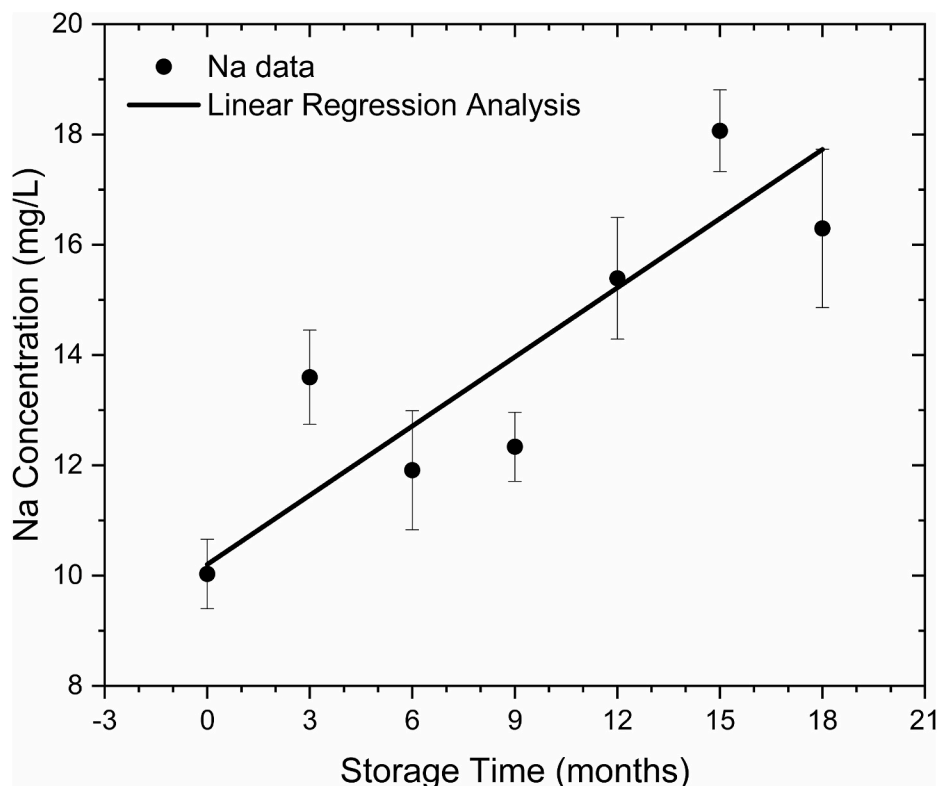


Fig. 5. Sodium concentration as a function of the storage time. The straight line is the result of a linear regression analysis of the data (black dots). The population slope was tested with the F test with a level of significance of 0.05.

concentrations in the bottom layer of the corks as well, thus suggesting that a dynamic transfer process of elements between the cork and the wine could be at play. One possible explanation for the increase of some elemental concentrations in sparkling white wine is the secondary fermentation process followed by wine aging. Once the secondary fermentation is completed, an autolysis process takes place and yeast cells start degrading over time releasing compounds and elements present in the cells to the beverage. The wine aging on yeast lees is therefore an important process to impart new features to the wine. Certainly, this proposed mechanism deserves further investigation.

Finally, Ba was not detected in any sample of the sparkling white wine, thus suggesting that Ba diffused to the bottom layer of the cork but

did not dissolve into the wine.

CRediT authorship contribution statement

Rafaela Debastiani: Sample preparation, Data acquisition, Formal analysis, Article preparation. **Carla Eliete Iochims dos Santos:** Sample preparation, Data acquisition, Formal analysis, Article preparation. **Johnny Ferraz Dias:** Project leader.

Declaration of competing interest

The authors declare that they have no known competing financial

Table 6
Elemental deposition rates in the sparkling wine.

Element	Deposition Rate (mg·L ⁻¹ ·month ⁻¹)
Na	0.42 ± 0.10
P	0.91 ± 0.54
S	2.68 ± 0.45
Cl	0.27 ± 0.07
K	13.6 ± 3.2
Ca	1.06 ± 0.24
Mn	0.032 ± 0.006
Fe	0.015 ± 0.006
Zn	0.016 ± 0.002
Rb	0.08 ± 0.02

interests or personal relationships that could have appeared to influence the work reported in this paper.

Acknowledgement

We thank the cooperation of Dr. V. Manfroi from the Institute of Science and Food Technology (Federal University of Rio Grande do Sul) and of Casa Valduga winery for providing the samples used in this work. This work was partially supported by CAPES (Coordenação de Aperfeiçoamento de Pessoal de Nível Superior) and CNPq (Conselho Nacional de Desenvolvimento Científico e Tecnológico). This project is part of the Coordinated Research Project F11021 sponsored by the International Atomic Energy Agency (IAEA) under contract number 21125.

References

- Campbell, J.L., Hopman, T.L., Maxwell, J.A., Nejedly, Z., 2000. The Guelph PIXE software package III: alternative proton database. *Nucl. Instrum. Methods Phys. Res. Sect. B Beam Interact. Mater. Atoms* 170 (1–2), 193–204. [https://doi.org/10.1016/S0168-583X\(00\)00156-7](https://doi.org/10.1016/S0168-583X(00)00156-7).
- Caniza, D.A.A., Turatti, A.M., Fernandes, F., Dias, J.F., dos Santos, C.E.I., 2020. Geochemical markers of *Ilex paraguariensis* determined by PIXE. *Nucl. Instrum. Methods Phys. Res. Sect. B Beam Interact. Mater. Atoms* 477, 163–168. <https://doi.org/10.1016/j.nimb.2019.10.015>.
- Cerdán, T.G., Goni, D.T., Azpilicueta, C.A., 2004. Accumulation of volatile compounds during ageing of two red wines with different composition. *J. Food Eng.* 65, 349–356. <https://doi.org/10.1016/j.jfoodeng.2004.01.032>.
- Chung, H.-J., Son, J.-H., Park, E.-Y., Lim, S.-T., 2008. Effect of vibration and storage on some physico-chemical properties of a commercial red wine. *J. Food Compos. Anal.* 21, 655–659. <https://doi.org/10.1016/j.jfca.2008.07.004>.
- Cloete, K.J., Šmit, Ž., Minnis-Ndimba, R., Vavpetić, P., du Plessis, A., le Roux, S.G., Pelicon, P., 2019. Physico-elemental analysis of roasted organic coffee beans from Ethiopia, Colombia, Honduras, and Mexico using X-ray micro-computed tomography and external beam particle induced X-ray emission. *Food Chem. X* 2, 100032. <https://doi.org/10.1016/j.fochx.2019.100032>.
- Corona, T., Iglesias, M., Anticó, E., 2014. Migration of components from cork stoppers to food: challenges in determining inorganic elements in food simulants. *J. Agric. Food Chem.* 62 (24), 5690–5698. <https://doi.org/10.1021/jf500170w>.
- Culbert, J.A., McRae, J.M., Condé, B.C., Schmidtke, L.M., Nicholson, E.L., Smith, P.A., Howell, K.S., Boss, P.K., Wilkinson, K.L., 2017. Influence of production method on the chemical composition, foaming properties, and quality of Australian carbonated and sparkling white wines. *J. Agric. Food Chem.* 65 (7), 1378–1386. <https://doi.org/10.1021/acs.jafc.6b05678>.
- Culbert, J., Cozzolino, D., Ristic, R., Wilkinson, K., 2015. Classification of sparkling wine style and quality by MIR spectroscopy. *Molecules* 20 (5), 8341–8356. <https://doi.org/10.3390/molecules20058341>.
- Debastiani, R., dos Santos, C.E.I., Ramos, M.M., Souza, V.S., Amaral, L., Dias, J.F., 2019a. Elemental extraction factor from ground to drinking coffee as a function of the water temperature. *Nucl. Instrum. Methods Phys. Res. B* 477, 154–158. <https://doi.org/10.1016/j.nimb.2019.11.026>.
- Debastiani, R., dos Santos, C.E.I., Ramos, M.M., Souza, V.S., Amaral, L., Yoneama, M.L., Dias, J.F., 2019b. Elemental analysis of Brazilian coffee with ion beam techniques: from ground coffee to the final beverage. *Food Res. Int.* 119, 297–304. <https://doi.org/10.1016/j.foodres.2019.02.007>.
- dos Santos, C.E.I., Debastiani, R., Souza, V.S., Peretti, D.E., Jobim, P.F., Yoneama, M.L., Amaral, L., Dias, J.F., 2019. The influence of the winemaking process on the elemental composition of the Marselan red wine. *J. Sci. Food Agric.* 99 (10), 4642–4650. <https://doi.org/10.1002/jsfa.9704>.
- dos Santos, C.E.I., da Silva, L.R.M., Bouffleur, L.A., Debastiani, R., Stefanon, C.A., Amaral, L., Yoneama, M.L., Dias, J.F., 2010. Elemental characterisation of cabernet sauvignon wines using particle-induced X-ray emission (PIXE). *Food Chem.* 121 (1), 244–250. <https://doi.org/10.1016/j.foodchem.2009.11.079>.
- dos Santos, C.E.I., Debastiani, R., Przybyłowicz, W., Manfroi, V., Amaral, L., Yoneama, M.L., Dias, J.F., 2013. Study of the elemental composition of wine stoppers using PIXE. *X Ray Spectrom.* 42 (3), 158–164. <https://doi.org/10.1002/xrs.2451>.
- EFSA, 2016a. Safety assessment of the active substance potassium metabisulfite, for use in active food contact materials. *EFSA Journal* 14 (5), 1–8. <https://doi.org/10.2903/j.efsa.2016.4465>.
- EFSA, 2016b. Scientific Opinion on the re-evaluation of sulfur dioxide (E 220), sodium sulfite (E 221), sodium bisulfite (E 222), sodium metabisulfite (E 223), potassium metabisulfite (E 224), calcium sulfite (E 226), calcium bisulfite (E 227) and potassium bisulfite. *EFSA Journal* 14 (4), 1–151. <https://doi.org/10.2903/j.efsa.2016.4438>.
- Fernandes, F., Niekraszewicz, L.A.B., Amaral, L., Dias, J.F., 2018. Evaluation of detector efficiency through GUPIXWIN H value. *Nucl. Instrum. Methods Phys. Res. Sect. B Beam Interact. Mater. Atoms* 417, 56–59. <https://doi.org/10.1016/j.nimb.2017.07.035>.
- Fornairon-Bonnefond, C., Camarasa, C., Moutounet, M., Salmon, J.M., 2002. New trends on yeast autolysis and wine ageing on lees: a bibliographic review. *J. Int. Sci. Vigne Vin* 36 (2), 49–69. <https://doi.org/10.20870/oeno-one.2002.36.2.974>.
- Giulian, R., dos Santos, C.E.I., Shubeita, S. de M., da Silva, L.M., Dias, J.F., Yoneama, M. L., 2007. Elemental characterization of commercial mate tea leaves (*Ilex paraguariensis* A. St.-Hil.) before and after hot water infusion using ion beam techniques. *J. Agric. Food Chem.* 55 (3), 741–746. <https://doi.org/10.1021/jf062456r>.
- Halász, A., László, R., 1991. Use of Yeast Biomass in Food Production. CRC Press, Inc. <https://doi.org/10.1201/9780203734551>.
- International Organisation of Vine and Wine, 2019. 2019 statistical report on world vitiviniculture. <http://www.oiv.int/public/medias/6782/oiv-2019-statistical-report-on-world-vitiviniculture.pdf>. (Accessed 21 January 2020).
- Jackson, D.I., Lombard, P.B., 1993. Environmental and management practices affecting grape composition and wine quality – a review. *Am. J. Enol. Vitic.* 44 (4), 409–430.
- Johansson, S.A.E., Campbell, J.L., Malmqvist, K.G., 1995. Particle-induced X-Ray Emission Spectrometry (PIXE). Wiley.
- Joshi, V.K., 2011. Handbook of Enology: Principles, Practices and Recent Innovations. Asiatech Publishers.
- Kemp, B., Condé, B., Jégou, S., Howell, K., Vasserot, Y., Marchal, R., 2019. Chemical compounds and mechanisms involved in the formation and stabilization of foam in sparkling wines. *Crit. Rev. Food Sci. Nutr.* 59 (13), 2072–2094. <https://doi.org/10.1080/10408398.2018.1437535>.
- Martínez-Lapuente, L., Apolar-Valiente, R., Guadalupe, Z., Ayestarán, B., Pérez-Magariño, S., Williams, P., Doco, T., 2018. Polysaccharides, oligosaccharides and nitrogen compounds change during the ageing of Tempranillo and Verdejo sparkling wines. *J. Sci. Food Agric.* 98 (1), 291–303. <https://doi.org/10.1002/jsfa.8470>.
- Mello, L. M. R. de, 2019. Vitivinicultura brasileira: panorama 2018, 12. <http://www.infoteca.cnptia.embrapa.br/infoteca/handle/doc/1113215>.
- NIH, 2020. National Institutes of Health, Office of Dietary Supplements. U.S. Department of Health & Human Services ods.od.nih.gov/HealthInformation/DietaryReferenceIntakes.aspx.
- Ortega-Fernández, C., González-Adrados, J.R., García-Vallejo, M.C., Calvo-Haro, R., Cáceres-Esteban, M.J., 2006. Characterization of surface treatments of cork stoppers by FTIR-ATR. *J. Agric. Food Chem.* 54 (14), 4932–4936. <https://doi.org/10.1021/jf0529823>.
- Rizzolo, R.G., Guerra, C.C., Perissutti, G.E., Ben, R.L., Navroski, R., Malgarim, M.B., 2018. Physicochemical and sensory characteristics of fine sparkling red wines produced at different maceration lengths in the south of Brazil. *Biosci. J.* 34 (1), 37–47. <https://doi.org/10.14393/BJ-v34n6a2018-39929>.
- Rizzon, L.A., Miele, A., Scopel, G., 2009. Analytical characteristics of Chardonnay wines from the Serra Gaúcha region. *Ciência Rural.* 39 (8), 2555–2558.
- Rizzon, L.A., Miele, A., 2009. Analytical characteristics of Merlot wines from the Serra Gaúcha region. *Ciência Rural.* 39 (6), 1913–1916. <https://doi.org/10.1590/s0103-84782009005000109>.
- Rodrigues, N.P., Rodrigues, E., Celso, P.G., Kahmann, A., Yamashita, G.H., Anzanello, M. J., Manfroi, V., Hertz, P.F., 2020. Discrimination of sparkling wines samples according to the country of origin by ICP-OES coupled with multivariate analysis. *LWT - Food Sci. Technol. (Lebensmittel-Wissenschaft -Technol.)* 131, 109760. <https://doi.org/10.1016/j.lwt.2020.109760>.
- Sartor, S., Toaldo, I.M., Panceri, C.P., Caliar, V., Luna, A.S., de Gois, J.S., Bordignon-Luiz, M.T., 2019. Changes in organic acids, polyphenolic and elemental composition of rosé sparkling wines treated with mannoproteins during over-lees aging. *Food Res. Int.* 124, 34–42. <https://doi.org/10.1016/j.foodres.2018.11.012>.
- Shahzamani, M., Rezaeian, I., Loghmani, M.S., Zahedi, P., Rezaeian, A., 2012. Effects of BaSO₄, CaCO₃, kaolin and quartz fillers on mechanical, chemical and morphological properties of cast polyurethane. *Plastics, Rubber and Composites* 41 (6), 263–269. <https://doi.org/10.1179/1743289811Y.0000000035>.
- Singh, S., Oswal, M., Behera, B.R., Kumar, A., Santra, S., Acharya, R., Singh, K.P., 2020. PIXE analysis of green and roasted coffee beans and filter coffee powder for the inter-comparison study of major, minor and trace elements. *AIP Conference Proceedings* 2220, 130032. <https://doi.org/10.1063/5.0001751>.
- Six, T., Feigenbaum, A., 2003. Mechanism of migration from agglomerated cork stoppers. Part 2: safety assessment criteria of agglomerated cork stoppers for champagne wine cork producers, for users and for control laboratories. *Food Addit. Contam.* 20 (10), 960–971. <https://doi.org/10.1080/02652030310001597583>.

Six, T., Feigenbaum, A., Riquet, A.-M., 2002. Mechanism of migration from agglomerated cork stoppers: I. An electron spin resonance investigation. *J. Appl. Polym. Sci.* 83 (12), 2644–2654. <https://doi.org/10.1002/app.10230>.

Yamada, E.A., Sgarbieri, V.C., 2005. Yeast (*Saccharomyces cerevisiae*) protein concentrate: preparation, chemical composition, and nutritional and functional

properties. *J. Agric. Food Chem.* 53 (10), 3931–3936. <https://doi.org/10.1021/jf0400821>.

Ziegler, J.F., 1977. The Stopping and Ranges of Ions in Matter. <https://doi.org/10.1016/C2013-0-00699-8>.